

The spectral properties of Fermi blazars: the spectral sequence and unification of blazars *

Luo-En Chen¹, Huai-Zhen Li¹, Ting-Feng Yi², Shu-Bai Zhou³ and Kai-Yi Li¹

¹ Physics Department, Yuxi Normal University, Yuxi 653100, China; lhz@yxnu.net

² Physics Department, Yunnan Normal University, Kunming 650092, China

³ Physics Department, Yunnan University, Kunming 650091, China

Received 2011 August 26; accepted 2012 July 17

Abstract Using a large sample of blazars of the Fermi observations presented by Abdo et al., we constructed a sample of blazars including high energy peaked BL Lac objects (HBLs), low energy peaked BL Lac objects (LBLs) and flat-spectral radio quasars (FSRQs). These unique characteristics make it possible to unambiguously address the question of how HBLs, LBLs and FSRQs are related. In this paper, we investigated the relationship between X-ray and γ -ray spectral indices ($\alpha_x-\alpha_\gamma$), as well as the relationship between the broadband spectral indices ($\alpha_{\text{ro}}-\alpha_{\text{rx}}$, $\alpha_{\text{ro}}-\alpha_{\text{ox}}$, $\alpha_{\text{ro}}-\alpha_{\text{x}\gamma}$ and $\alpha_{\text{rx}}-\alpha_{\text{x}\gamma}$) for this sample. The color-color diagram shows that there is a significant correlation between both quantities when all three subclasses of blazars are considered, which suggests that there is a unified scheme for blazars. On the other hand, the $\alpha_x-\alpha_\gamma$ diagram reveals that three kinds of blazars have different spectral energy distributions: the trend of HBLs is different from that of FSRQs and LBLs, whereas FSRQs and LBLs have a similar trend, which hints that FSRQs and LBLs have similar spectral properties, but HBLs have distinct spectral properties. In addition, the broadband energy distributions also reveal the similar spectral properties with that of the $\alpha_x-\alpha_\gamma$ diagram. The spectral properties revealed from the Fermi sample do not support the blazar sequence reported by Fossati et al. and Ghisellini et al.

Key words: galaxies: active — BL Lacertae objects: general — galaxies: fundamental parameters — quasars: general

1 INTRODUCTION

Blazars are the most interesting subclasses of active galactic nuclei (AGNs), because they are the brightest and most variable high energy sources among AGNs, and have continuous spectral energy distributions (SEDs). The nonthermal continuum emission of blazars extends up to X-ray and γ -ray frequencies. In general, blazars are comprised of flat-spectral radio quasars (FSRQs) and BL Lac objects. The chief difference between these two classes lies in properties of their optical emission lines: BL Lac objects are characterized by the lack of strong emission lines (equivalent width $< 5 \text{ \AA}$), while FSRQs have strong broad emission lines with similar strength to normal quasars (Scarpa & Falomo 1997). In addition, the BL Lac objects can be divided into two subclasses: “high energy peaked BL

* Supported by the National Natural Science Foundation of China.

Lac objects” (HBLs) and “low energy peaked BL Lac objects” (LBLs) (Giommi et al. 1995). The relationship between HBLs and LBLs has been investigated by many authors (e.g. Giommi et al. 1990; Giommi & Padovani 1994; Giommi et al. 1995; Lamer et al. 1996; Padovani & Giommi 1995, 1996; Schachter et al. 1993; Stocke et al. 1985, 1991; Urry & Padovani 1995), who found that both subclasses have different SEDs.

BL Lac objects and FSRQs are grouped together under the denomination of blazars, which eliminate the somewhat ambiguous issue of the strength of the emission lines as a classification criterion. However, there are some differences in the individual emission properties among different blazar subclasses. The relationship, especially the SEDs, among three kinds of blazars can promote our understanding of the fundamental properties of blazars. Therefore, it is important to investigate the connection among FSRQs, LBLs and HBLs. The SEDs of blazars have been studied by many authors (Antón & Browne 2005; Comastri et al. 1997; Foschini et al. 2006; Fossati et al. 1998; Ghisellini et al. 1998, 2009; Sambruna et al. 1996; Padovani 2007; Xie et al. 2001a,b, 2003, 2006, 2007, 2008; Zheng et al. 2007), who found different results for the relationship between different kinds of blazars.

Based on the classical samples, Fossati et al. (1998) and Ghisellini et al. (1998) compared the SEDs of the different subclasses of blazars, and found that the continuum shapes of the different subclasses of blazars are different, but the SEDs of these subclasses exhibit a remarkable continuity and follow a unified scheme. Sambruna et al. (1996) and Xie et al. (2003) also investigated the multifrequency spectral properties of three different kinds of blazars, and the results supported the blazar sequence. However, Antón & Browne (2005) and Padovani (2007) found that their sample did not follow the blazar sequence reported by Fossati et al. (1998) and Ghisellini et al. (1998). They suggested that there are selection effects for the systematic trend (Antón & Browne 2005; Padovani 2007). Nieppola et al. (2006) found the correlation between luminosities and the synchrotron peak frequency ν_{peak} is negative in radio and optical bands, whereas in X-rays the correlation turns slightly positive, which is not consistent with a “blazar sequence.” Li et al. (2010) studied the relationship among the different kinds of blazars and found that the trend of HBLs in the color-color diagram is different from that of LBLs and FSRQs. In addition, Padovani (2007) reviewed the validity of the blazar sequence and found that the blazar sequence, in its simplest form, is ruled out.

The continuum emission of blazars is produced by a relativistic jet oriented close to the observer emanating from the vicinity of a black hole (Stern & Poutanen 2008; Ghisellini et al. 1986). The SEDs of blazars from radio to γ -ray energies are characterized by a universal structure with two bumps, which can be accounted for via the synchrotron self-Compton processes (SSC model) (Cui 2009). The lower-energy peak can be explained by synchrotron radiation, while the high-energy γ -ray emission can be accounted for by inverse Compton processes (Sambruna et al. 1996).

In order to reassess the properties of blazars, in this paper, we study the radio-optical-X-ray- γ -ray SEDs of Fermi blazars and connections among LBLs, HBLs and FSRQs, which can improve our understanding about the relationship among different subclasses of blazars and the nature of blazars. The plan for the paper is as follows: Section 2 gives the Fermi sample and Section 3 presents the results of the analysis on the collected data. A general discussion and conclusions are given in Section 4.

2 THE SAMPLE OF FERMI BLAZARS

The Large Area Telescope (LAT) onboard the Fermi Gamma Ray Space Telescope provides unprecedented sensitivity in the γ -ray band (Atwood et al. 2009) and has started producing large and homogeneous samples of blazars. The first Fermi sample revealed more than one hundred blazars with γ -ray luminosity and photon spectral index Γ_{γ} (Abdo et al. 2009). Based on the first Fermi sample and the literatures (Li et al. 2010; Abdo et al. 2010a), we compiled a sample of 66 blazars which have X-ray spectral index α_x . Among them, 13 are HBLs, 23 are LBLs and 30 are FSRQs.

The data used in our paper are obtained from the Fermi, Swift, radio/mm telescopes and optical facilities with a large number of multifrequency simultaneous or quasi-simultaneous observations (Abdo et al. 2010a). The broadband spectral indices α_{ro} , α_{rx} , α_{ox} and $\alpha_{\text{x}\gamma}$ are computed using the flux at rest frame 5 GHz, 5000 Å, 1 keV and 100 MeV, respectively. Moreover, the values of these spectral indices are also given by Abdo et al. (2010a). The γ -ray spectral index α_{γ} is presented from Abdo et al. (2009). In addition, the classes and the X-ray spectral index α_{x} are based on the sample of Li et al. (2010) and Abdo et al. (2010a).

The relevant data for 66 blazars are listed in Table 1 as follows: Column (1): the LAT name; Column (2): other name of the sample; Column (3): the redshift z ; Column (4): the class of the source; high energy peaked BL Lac objects, low energy peaked BL Lac objects and flat spectrum radio quasars are labeled with HBL, LBL and FSRQ, respectively; Column (5): the radio-to-optical spectral index α_{ro} ; Column (6): the radio-to-X-ray spectral index α_{rx} ; Column (7): the optical-to-X-ray spectral index α_{ox} ; Column (8): X-ray-to- γ -ray spectral index $\alpha_{\text{x}\gamma}$; Column (9): X-ray spectral index α_{x} ; Column (10): γ -ray spectral index α_{γ} .

3 SPECTRAL ENERGY DISTRIBUTIONS OF FERMI BLAZARS

In order to reassess the relationship among three subclasses of blazars and improve our understanding of the fundamental properties of blazars, we analyzed the SEDs of Fermi blazars following two approaches. The first is to investigate the X-ray and γ -ray energy distribution of three kinds of blazars, and the second is to compute the broadband spectral indices.

3.1 X-ray and γ -ray Energy Distribution

In Figure 1, we plot α_{x} versus α_{γ} for our sample. Figure 1 shows that FSRQs and HBLs have a distinct distribution of α_{x} , which reveals that they have different spectral properties in X-ray. The distribution of α_{x} for LBLs is overlapped with that of FSRQs and HBLs. Moreover, Figure 1 also shows that the distribution of the three classes along the vertical axis is completely distinct: they, from HBLs to LBLs to FSRQs, have an increasing value of α_{γ} , which hints that three kinds of blazars have different spectral properties in γ -ray.

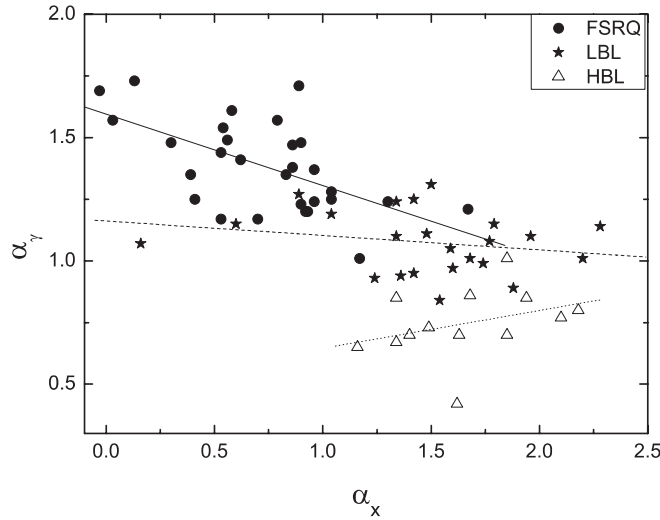


Fig. 1 α_{x} versus α_{γ} for three subclasses of Fermi blazars.

Table 1 The Sample of Fermi Blazars

LAT name	Other name	z	Class	α_{ro}	α_{rx}	α_{ox}	$\alpha_{\text{x}\gamma}$	α_{x}	α_{γ}
OFGL J0033.6-1921	1RXS J003334.6-1	0.61	HBL	0.23	0.53	1.08	1.04	1.4	0.7
OFGL J0050.5-0928	PKS 0048-09		LBL	0.52	0.84	1.46	0.72	1.79	1.15
OFGL J0112.1+2247	GC 0109+224		LBL	0.33	0.79	1.67	0.74	1.96	1.1
OFGL J0120.5-2703	1Jy0118-272	0.557	LBL	0.49	0.91	1.66	0.74	1.74	0.99
OFGL J0136.6+3903	1RXS J013632.9+3		HBL	0.24	0.59	1.28	1.04	1.16	0.65
OFGL J0137.1+4751	S40133+47	0.859	FSRQ	0.71	0.93	1.25	0.64	0.92	1.2
OFGL J0204.8-1704	PKS 0202-17	1.74	FSRQ	0.71	0.94	1.3	0.57	0.3	1.48
OFGL J0210.8-5100	PKS 0208-512	1.003	FSRQ	0.59	0.97	1.66	0.54	1.04	1.28
OFGL J0222.6+4302	3C 66A	0.444	LBL	0.41	0.84	1.68	0.66	1.6	0.97
OFGL J0229.5-3640	PKS 0227-369	2.115	FSRQ	0.76	0.82	0.82	0.53	0.03	1.57
OFGL J0238.4+2855	4C28.07	1.213	FSRQ	0.86	0.98	1.13	0.59	0.56	1.49
OFGL J0238.6+1636	PKS 0235+164	0.94	LBL	0.75	0.92	1.15	0.51	1.59	1.05
OFGL J0303.7-2410	PKS 0301-243	0.26	LBL	0.43	0.74	1.33	0.9	1.68	1.01
OFGL J0334.1-4006	PKS 0332-403		LBL	0.71	0.93	1.34	0.68	0.6	1.15
OFGL J0423.1-0112	PKS 0420-01	0.916	FRSQ	0.73	0.96	1.31	0.68	0.86	1.38
OFGL J0428.7-3755	PKS 0426-380	1.03	LBL	0.54	0.95	1.61	0.5	2.28	1.14
OFGL J0449.7-4348	PKS 0447-439	0.205	HBL	0.35	0.69	1.35	0.83	1.85	1.01
OFGL J0457.1-2325	PKS 0454-234	1.003	FSRQ	0.79	0.97	1.26	0.46	0.9	1.23
OFGL J0507.9+6739	1ES0502+675	0.416	HBL	0.3	0.54	0.97	1.07	1.34	0.67
OFGL J0531.0+1331	PKS 0528+134	2.07	FSRQ	0.75	0.97	1.2	0.53	0.54	1.54
OFGL J0538.8-4403	PKS 0537-441	0.892	LBL	0.64	0.94	1.41	0.6	1.04	1.19
OFGL J0722.0+7120	S50716+714		LBL	0.39	0.84	1.71	0.69	1.77	1.08
OFGL J0730.4-1142	PKS 0727-11	1.589	FSRQ	0.87	1.03	1.19	0.48	0.72	-
OFGL J0738.2+1738	PKS 0735+17	0.424	LBL	0.47	0.93	1.78	0.72	1.34	1.1
OFGL J0818.3+4222	S4 0814+425	0.53	LBL	0.88	0.99	1.11	0.56	0.16	1.07
OFGL J0855.4+2009	PKS 0851+202	0.306	LBL	0.49	0.92	1.69	0.7	1.5	1.31
OFGL J0921.2+4437	S40917+44	2.19	FSRQ	0.85	0.89	0.89	0.65	0.39	1.35
OFGL J0957.6+5522	4C55.17	0.896	FSRQ	0.73	0.97	1.41	0.62	1.17	1.01
OFGL J1015.2+4927	1H 1013+498	0.2	HBL	0.38	0.68	1.23	0.98	1.49	0.73
OFGL J1053.7+4926	WE 1050+49W1	0.14	HBL	0.14	0.74	1.9	0.98	1.62	0.42
OFGL J1057.8+0138	4C01.28	0.888	FSRQ	0.75	0.96	1.27	0.72	0.93	1.2
OFGL J1058.9+5629	RXJ10586+5628	0.143	LBL	0.28	0.75	1.65	0.84	1.48	1.11
OFGL J1104.5+3811	MKN421	0.03	HBL	-0.08	0.58	1.86	1.1	2.1	0.77
OFGL J1129.8-1443	PKS 1127-145	1.184	FSRQ	0.72	0.95	1.37	0.65	-0.03	1.69
OFGL J1146.7-3808	PKS 1144-379	1.048	FSRQ	0.6	0.93	1.53	0.69	1.67	1.21
OFGL J1159.2+2912	4C29.45	0.729	FSRQ	0.67	0.92	1.4	0.61	0.86	1.47
OFGL J1218.0+3006	ON 325	0.13	LBL	0.38	0.67	1.21	0.96	1.88	0.89
OFGL J1221.7+2814	ON 231	0.102	LBL	0.23	0.88	2.14	0.71	1.24	0.93
OFGL J1229.1+0202	3C273	0.158	FSRQ	0.76	0.87	1.09	0.8	0.89	1.71
OFGL J1246.6-2544	PKS 1244-255	0.635	FSRQ	0.67	0.92	1.33	0.7	1.3	1.24
OFGL J1248.7+5811	PG 1246+586		LBL	0.35	0.76	1.55	0.87	1.42	0.95
OFGL J1256.1-0547	3C279	0.536	FSRQ	0.71	0.86	1.1	0.8	0.83	1.35
OFGL J1310.6+3220	1Jy1308+326	0.997	FSRQ	0.92	0.95	0.97	0.55	1.04	1.25
OFGL J1355.0-1044	PKS 1352-104	0.33	FSRQ	0.6	0.84	1.27	0.72	0.96	1.37
OFGL J1427.1+2347	PG 1424+240		HBL	0.34	0.76	1.57	0.84	2.18	0.8
OFGL J1457.6-3538	BZQ J1457-3539	1.424	FSRQ	0.77	0.9	1.09	0.47	0.96	1.24
OFGL J1504.4+1030	PKS 1502+106	1.839	FSRQ	0.92	1.04	1.16	0.31	0.53	1.17
OFGL J1512.7-0905	PKS 1510-08	0.36	FSRQ	0.61	0.93	1.54	0.49	0.9	1.48
OFGL J1517.9-2423	APLIB	0.048	LBL	0.33	0.93	2.09	0.75	1.36	0.94
OFGL J1555.8+1110	PG 1553+113		HBL	0.34	0.69	1.39	0.97	1.85	0.7
OFGL J1635.2+3809	4C38.41	1.814	FSRQ	0.78	1.06	1.49	0.41	0.53	1.44
OFGL J1653.9+3946	MKR501	0.033	HBL	-0.03	0.71	2.13	1.11	1.63	0.7
OFGL J1719.3+1746	PKS 1717+177	0.137	LBL	0.62	0.92	1.47	0.62	1.54	0.84
OFGL J1751.5+0935	OT 081	0.322	LBL	0.65	0.93	1.4	0.6	0.89	1.27
OFGL J1802.2+7827	S51803+784	0.68	LBL	0.6	0.96	1.57	0.67	1.42	1.25
OFGL J1849.4+6706	4C66.20	0.657	FSRQ	0.66	0.93	1.39	0.53	0.7	1.17
OFGL J2000.2+6506	1ES1959+650	0.047	HBL	0.08	0.61	1.64	1.06	1.68	0.86
OFGL J2009.4-4850	1Jy2005-489	0.071	HBL	0.16	0.7	1.75	1.09	1.94	0.85
OFGL J2139.4-4238	MH 2136-428		LBL	0.34	0.78	1.64	0.66	2.2	1.01
OFGL J2143.2+1741	S32141+17	0.213	FSRQ	0.43	0.92	1.85	0.56	0.79	1.57
OFGL J2158.8-3014	PKS 2155-304	0.116	HBL	0.22	0.51	1.07	1.13	1.34	0.85
OFGL J2202.4+4217	BLLAC	0.069	LBL	0.29	0.93	2.17	0.7	1.34	1.24
OFGL J2203.2+1731	PKS 2201+171	1.076	FSRQ	0.81	0.93	1.06	0.61	0.41	1.25
OFGL J2232.4+1141	4C-11.69	1.037	FSRQ	0.77	0.96	1.32	0.61	0.58	1.61
OFGL J2254.0+1609	3C454.3	0.859	FSRQ	0.58	0.93	1.55	0.53	0.62	1.41
OFGL J2327.3+0947	PKS 2325+093	1.843	FSRQ	0.77	0.89	1.04	0.54	0.13	1.73

Table 2 Statistical Results for the Sample of Fermi Blazars

Relation	Source type	Objects	Slope	Correlation coeff.	Chance probability
$\alpha_x - \alpha_\gamma$	Blazar	65	-0.35	-0.69	$p < 10^{-4}$
$\alpha_x - \alpha_\gamma$	FSRQ	29	-0.29	-0.59	$p = 7.8 \times 10^{-4}$
$\alpha_x - \alpha_\gamma$	LBL	23	-0.06	-0.22	$p = 0.31$
$\alpha_x - \alpha_\gamma$	HBL	13	0.15	0.34	$p = 0.25$
$\alpha_{ro} - \alpha_{rx}$	Blazar	66	0.43	0.79	$p < 10^{-4}$
$\alpha_{ro} - \alpha_{ox}$	FSRQ&LBL	53	-1.33	-0.82	$p < 10^{-4}$
$\alpha_{ro} - \alpha_{ox}$	HBL	13	-1.77	-0.72	$p = 0.006$
$\alpha_{ro} - \alpha_{x\gamma}$	Blazar	66	-0.65	-0.81	$p < 10^{-4}$
$\alpha_{rx} - \alpha_{x\gamma}$	Blazar	66	-1.31	-0.89	$p < 10^{-4}$

Interestingly, one can find that the spectral trend in the $\alpha_x - \alpha_\gamma$ plane is different for three kinds of blazars: FSRQs and LBLs have a negative spectral trend, but the trend becomes positive for HBLs. The negative spectral trend of FSRQs and LBLs revealed from Figure 1 implies that FSRQs and LBLs have similar spectral properties, which is consistent with the results reported by other authors (e.g. Fossati et al. 1998; Ghisellini et al. 1998; Li et al. 2010; Xie et al. 2003). In addition, the distribution of FSRQs and LBLs in the $\alpha_x - \alpha_\gamma$ diagram shows that there is a continuous trend going from FSRQs to LBLs, which provides more evidence or at least gives some hints for the conclusion of the unified scheme and the spectral sequence. The distinct spectral trend of HBLs suggests that HBLs have different spectral properties from the other kinds of blazars, which supports the conclusions reported by a number of authors (e.g. Li et al. 2010; Antón & Browne 2005) who found HBLs do not follow the spectral sequence reported by Fossati et al. (1998) and Ghisellini et al. (1998).

Although three kinds of blazars have different spectral properties, Figure 1 also shows that there is a good anticorrelation between both quantities when all three subclasses of blazars are considered. This is consistent with the correlation reported by Comastri et al. (1997) and Wang et al. (1996). The linear regression analysis equation is

$$\log \alpha_\gamma = -(0.35 \pm 0.05)\alpha_x + (1.56 \pm 0.06). \quad (1)$$

In this case the correlation coefficient is $r = -0.69$ and the chance probability is $p < 10^{-4}$. The significant correlation between α_x and α_γ suggests that similar physical processes operate in all objects, which is consistent with the previous results using other spectral parameters reported by many authors (e.g. Fossati et al. 1998; Ghisellini et al. 1998; Li et al. 2010; Xie et al. 2003; Zheng et al. 2007). The significant negative correlation revealed from Figure 1 supports the previous conclusions that there is a unified scheme for blazars. The significance of correlation and slopes of the linear regression for the samples are listed in Table 2. In Figure 2, we plot the number distributions of α_x and α_γ for the subsamples. The distributions are similar to those in Abdo et al. (2009).

3.2 Broadband Energy Distribution

Two-point (composite) spectral indices can be calculated following the formula (Ledden & Odell 1985)

$$\alpha_{12} = -\frac{\log(F_1/F_2)}{\log(\nu_1/\nu_2)}, \quad (2)$$

where F_1 and F_2 are the flux densities at frequencies ν_1 and ν_2 , respectively. For all the objects in our sample, the two-point spectral radio-to-optical (α_{ro}), radio-to-X-ray (α_{rx}), optical-to-X-ray (α_{ox}) and X-ray-to- γ -ray ($\alpha_{x\gamma}$) indices are computed using the flux densities at 5 GHz, 5000Å, 1 keV and 100 MeV respectively that have been k -corrected.

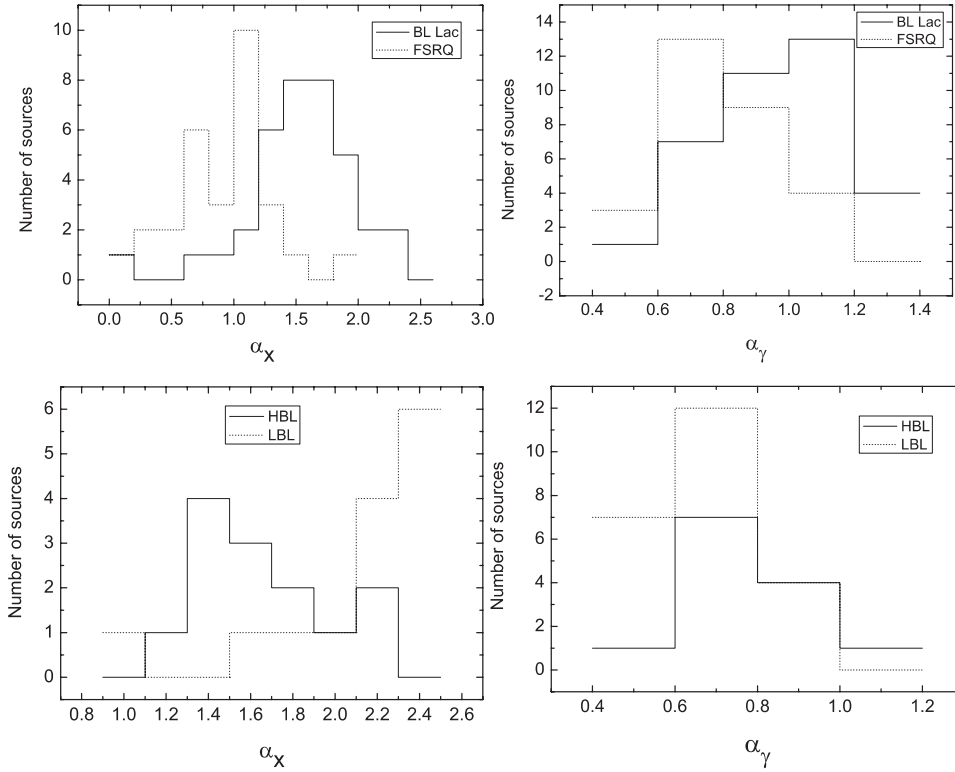


Fig. 2 Number distributions of α_X and α_γ for the blazar subsamples.

Figure 3 plots the broadband energy distributions (α_{TO} versus α_{TX} , α_{TO} versus α_{OX} , α_{TO} versus $\alpha_{X\gamma}$ and α_{TX} versus $\alpha_{X\gamma}$) of our samples, which shows a similar result as that obtained from Figure 1. From Figure 2, one can find that FSRQs and LBLs almost mix together, but HBLs occupy distinct regions in the color-color diagrams, which suggests FSRQs and LBLs have similar spectral properties, and HBLs have different spectral properties from FSRQs and LBLs. This is consistent with the previous results (e.g. Li et al. 2010; Xie et al. 2003). On the other hand, a good correlation between α_{TO} and α_{TX} , with correlation coefficient of $r = 0.79$ and chance probability of $p < 10^{-4}$, is revealed by the $\alpha_{\text{TO}}-\alpha_{\text{TX}}$ diagram, which is in good agreement with the conclusions about a unified model of blazars (see. Fossati et al. 1998; Ghisellini et al. 1998; Li et al. 2010; Sambruna et al. 1996; Xie et al. 2003). In addition, there is also a significant anticorrelation between α_{TO} and $\alpha_{X\gamma}$ with correlation coefficient of $r = -0.81$ and chance probability of $p < 10^{-4}$, as well as between α_{TX} and $\alpha_{X\gamma}$ with correlation coefficient of $r = -0.89$ and chance probability of $p < 10^{-4}$, which is consistent with the result revealed by the $\alpha_{\text{TO}}-\alpha_{\text{TX}}$ diagram and Figure 1. The correlations revealed from the broadband energy distributions provide more evidence, or at least provide some hints, for the unified blazar model.

4 DISCUSSION AND CONCLUSIONS

On the basis of ROSAT PSPC data for 27 bright EGRET and Whipple sources, Comastri et al. (1997) studied the relationship between BL Lac objects and FSRQs. They discovered that there is a significant anticorrelation between X-ray and γ -ray spectral indices, and also between the broadband spectral indices α_{TO} and $\alpha_{X\gamma}$. The correlation between the broadband spectral indices obtained by

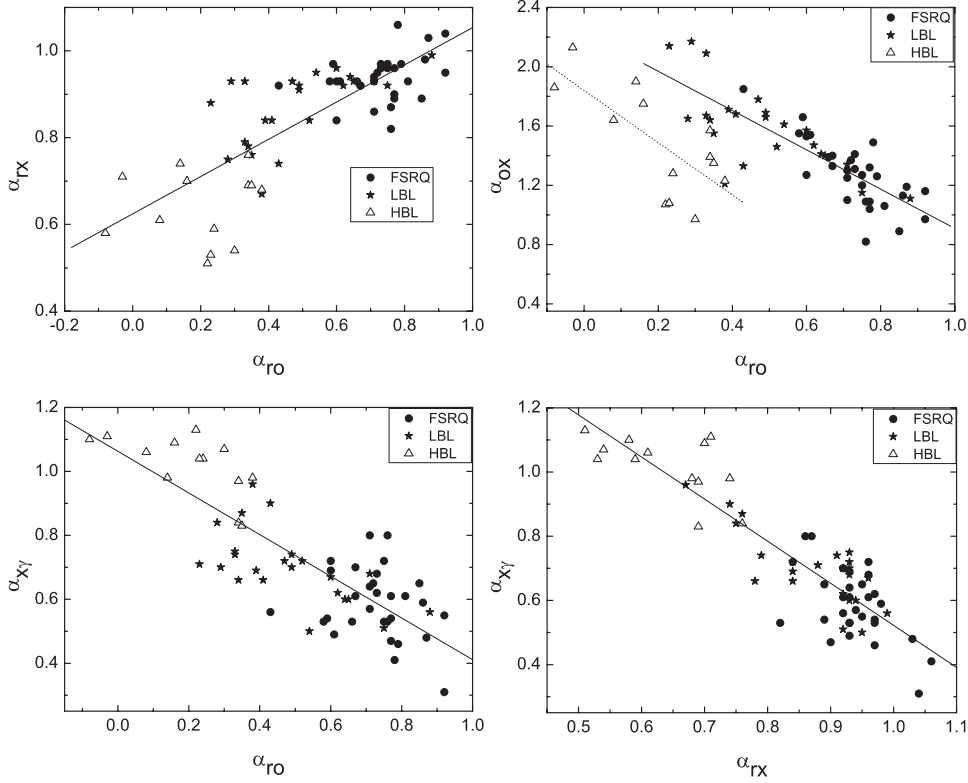


Fig. 3 Broadband energy distribution of Fermi blazars.

Comastri et al. (1997) implied that there is a different shape in overall energy distributions from radio to γ -ray energies between BL Lacs and FSRQs. They also found that the synchrotron peak energy of BL Lac objects is larger than that of FSRQs, which suggests that the synchrotron peak energy is an important parameter in describing the observed broadband energy distributions (Comastri et al. 1997). Maraschi et al. (2008) found that blazars exhibit a trend of increasing peak frequency with increasing luminosity, which is contrary to the blazar sequence reported by Fossati et al. (1998) and Ghisellini et al. (1998). They suggested that the spectral sequence applies only to average states (Maraschi et al. 2008).

In this paper, we have compiled the radio, optical, X-ray and γ -ray data for a new sample including 66 Fermi blazars and investigated the relationship among HBLs, LBLs and FSRQs. From Figures 1 and 2, a significant correlation is revealed, which suggests that similar physical processes operate in all objects. This is consistent with the previous conclusion reported by some authors (Comastri et al. 1997; Fossati et al. 1998; Ghisellini et al. 1998; Li et al. 2010; Sambruna et al. 1996; Xie et al. 2001a,b, 2003). This provides more evidence, or at least provides some hints, for the unified model of blazars. On the other hand, the spectral distribution revealed from Figure 1 suggests that the spectral trend of HBLs is different from that of FSRQs and LBLs, and there is a continuous trend going from FSRQs to LBLs. In addition, the broadband energy distributions also show that the spectral properties of HBLs are different from those of FSRQs and LBLs, which is consistent with the results revealed by Figure 1 and some of the previous results (e.g. Ant3n & Browne 2005; Li et al. 2010; Padovani 2007; Padovani et al. 2003; Xie et al. 2003). This implies that the results

presented by the Fermi sample do not support the blazar sequence reported by Fossati et al. (1998) and Ghisellini et al. (1998).

For the different results between the Fermi sample and the previous combined surveys, one important reason is that all the samples used by Fossati et al. (1998) are classic, high flux limit surveys in the radio and X-ray. This suggests there are selection effects for the results of the spectral sequence reported by Fossati et al. (1998), which is based on all available blazar SEDs taken from a whole range of samples with different selection criteria (Antón & Browne 2005). The different selection criteria lead to their sampling parameter spaces being less homogeneous and discontinuous, which would cause the biased result (Chen et al. 2006). In addition, the sample used by Xie et al. (2003) is rather small and only is comprised of four HBLs, which are difficult to use to completely confirm the spectral trend of HBLs. So, a large, homogeneous and well defined sample is necessary for a relatively unbiased view of blazar properties. Padovani et al. (2003) selected the Deep X-Ray Radio Blazar Survey (DXRBS) sample to test the blazar sequence, and found their results are contrary to the predictions of the blazar sequence scenario.

Fermi provides an unprecedented sensitivity in the γ -ray band with a large increase over its predecessors (Atwood et al. 2009; Thompson et al. 1993; Tavani et al. 2008). In addition, Fermi has produced a large and homogeneous sample of blazars, which is useful to reassess the issue of blazar properties (Abdo et al. 2010a). Obviously, our sample is produced based on a large and homogeneous sample with an unprecedented sensitivity in the γ -ray band. Moreover, other data used in our paper are obtained from the Swift, radio/mm telescopes and optical facilities that also have a high sensitivity. The selection effects of our samples are weak, as shown in Figure 4. In addition, in this paper, we investigated the spectral properties of blazars using a large number of multifrequency simultaneous or quasi-simultaneous observations. This would lead to a more unbiased view of blazar properties. Our analysis results seem to provide more evidence, or at least hints to argue, for what was reported by Li et al. (2010) and Padovani (2007). In the framework of the unified scheme of blazars, there are also different SEDs for different subclasses of blazars: HBLs follow a distinct trend from FSRQs and LBLs. Namely, the results presented by the Fermi sample provide more evidence for the unified blazar model reported by Fossati et al. (1998) and Ghisellini et al. (1998), but the results do not support the blazar spectral sequence reported by them.

The different SEDs between HBLs, LBLs and FSRQs may be related to the different X-ray spectra, the intrinsically different environments around the blazar's nucleus and the difference in the location of the emitting region. The X-ray spectra of LBLs and FSRQs are dominated by the inverse Compton emission of low-energy electrons, which lead to flat X-ray spectra for FSRQs and LBLs. However, HBLs have steep X-ray spectra, which are due to the fact that the X-ray spectra of HBLs are fully dominated by the synchrotron emission of very high energy electrons. In addition, Abdo et al. (2010a) found that FSRQs and LBLs are the low synchrotron peaked blazars, and the synchrotron peak frequencies of FSRQs and LBLs are lower than those of HBLs. Abdo et al. (2010b) found that a weak "harder when brighter" effect is apparent in LBLs and FSRQs, whereas no significant effect is present for HBLs. Moreover, Costamante (2009) found that a clear, physical difference is present in FSRQs and HBLs: compared with FSRQs, HBLs have a much "cleaner" environment. In addition, FSRQs and HBLs have very different emitting regions (Costamante 2009). The emitting region of FSRQs cannot be too close to the nucleus, whereas it likely located very close to the black hole for HBLs (Costamante 2009). All of these can lead to different spectral properties for the three kinds of blazars.

The unified model of AGNs is based on the accreting black hole system. The emission of a blazar is usually associated with the stream of a relativistic jet, and the overall spectrum is determined by the energy spectrum of the electrons as well as by the variation of the physical quantities along the jet (Begelman et al. 1984). Our results reveal that there are similar physical processes operating in all three kinds of blazars under a range of intrinsic physical conditions or the beaming parameter. However, our results also suggest that the three subclasses of blazars have different spectral distribu-

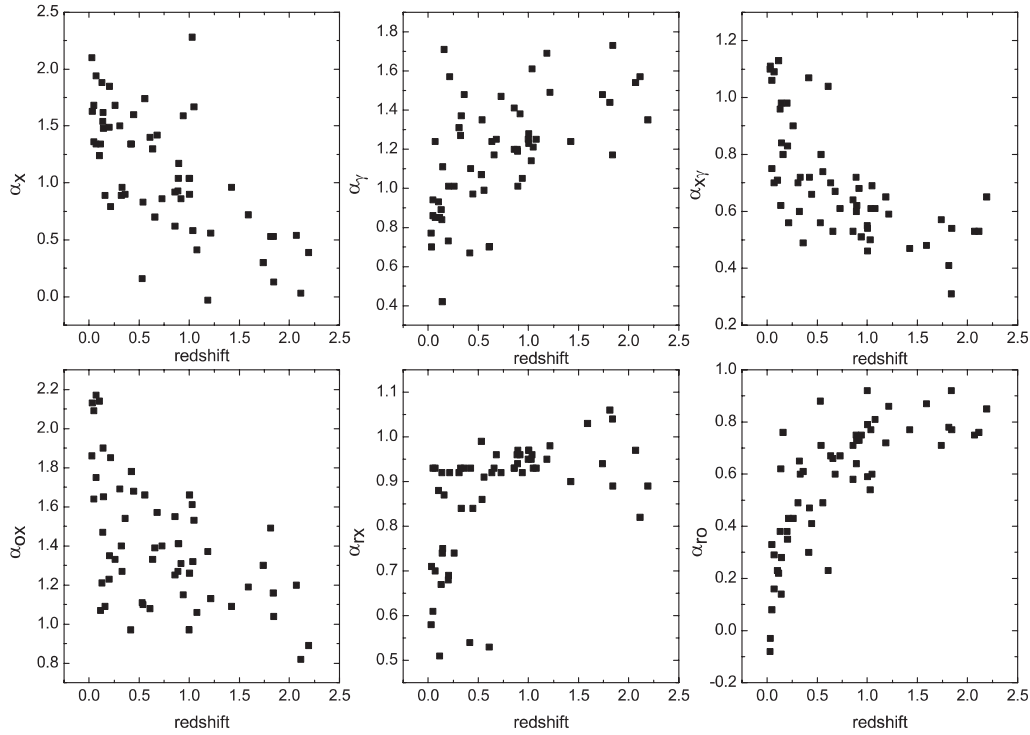


Fig. 4 Relations between redshift and spectral indices.

tions, which may be due to the different intrinsic environments around the blazar's nucleus and the different locations of the emitting region. On the other hand, the spectral indices are closely related to the indices of the electron energy distribution (Zhang et al. 2010). So one may speculate that the electron energy distributions of the FRSQs may be systematically different from those of BL Lacs. The difference in spectral index could be related to the different accretion modes in FRSQs and BL Lacs, so the accretion modes may be different in FRSQs and BL Lacs (Cao 2003; Xu et al. 2009). Despite the spectral energy distributions (SEDs) being strongly jet-dominated, in the coupled jet-disk accretion model, interactions between the jet and accretion disk are strong, and jet spectra can be modified by the accretion disk.

Acknowledgements We are grateful to anonymous referees for their constructive suggestions and valuable remarks to improve the manuscript. This work is supported by the National Natural Science Foundation of China (Grant No. 10878013), the Natural Science Foundation of Yunnan Province (2007A230M, 2011FZ081) and the Program for Innovative Research Team (in Science and Technology) in University of Yunnan Province (IRTSTYN).

References

- Abdo, A. A., Ackermann, M., Ajello, M., et al. 2009, *ApJ*, 700, 597
 Abdo, A. A., Ackermann, M., Agudo, I., et al. 2010a, *ApJ*, 716, 30
 Abdo, A. A., Ackermann, M., Ajello, M., et al. 2010b, *ApJ*, 710, 1271
 Antón, S., & Browne, I. W. A. 2005, *MNRAS*, 356, 225
 Atwood, W. B., Abdo, A. A., Ackermann, M., et al. 2009, *ApJ*, 697, 1071

- Begelman, M. C., Blandford, R. D., & Rees, M. J. 1984, *Reviews of Modern Physics*, 56, 255
- Cao, X. 2003, *ApJ*, 599, 147
- Chen, L. E., Xie, G. Z., Ren, J. Y., Zhou, S. B., & Ma, L. 2006, *ApJ*, 637, 711
- Comastri, A., Fossati, G., Ghisellini, G., & Molendi, S. 1997, *ApJ*, 480, 534
- Costamante, L. 2009, *International Journal of Modern Physics D*, 18, 1483
- Cui, W. 2009, *RAA (Research in Astronomy and Astrophysics)*, 9, 841
- Foschini, L., Ghisellini, G., Raiteri, C. M., et al. 2006, *A&A*, 453, 829
- Fossati, G., Maraschi, L., Celotti, A., Comastri, A., & Ghisellini, G. 1998, *MNRAS*, 299, 433
- Ghisellini, G., Celotti, A., Fossati, G., Maraschi, L., & Comastri, A. 1998, *MNRAS*, 301, 451
- Ghisellini, G., Maraschi, L., & Tavecchio, F. 2009, *MNRAS*, 396, L105
- Ghisellini, G., Maraschi, L., Treves, A., & Tanzi, E. G. 1986, *ApJ*, 310, 317
- Giommi, P., Ansari, S. G., & Micol, A. 1995, *A&AS*, 109, 267
- Giommi, P., Barr, P., Pollock, A. M. T., Garilli, B., & Maccagni, D. 1990, *ApJ*, 356, 432
- Giommi, P., & Padovani, P. 1994, *MNRAS*, 268, L51
- Lamer, G., Brunner, H., & Staubert, R. 1996, *A&A*, 311, 384
- Ledden, J. E., & Odell, S. L. 1985, *ApJ*, 298, 630
- Li, H. Z., Xie, G. Z., Yi, T. F., Chen, L. E., & Dai, H. 2010, *ApJ*, 709, 1407
- Maraschi, L., Ghisellini, G., Tavecchio, F., Foschini, L., & Sambruna, R. M. 2008, *International Journal of Modern Physics D*, 17, 1457
- Nieppola, E., Tornikoski, M., & Valtaoja, E. 2006, *A&A*, 445, 441
- Padovani, P. 2007, *Ap&SS*, 309, 63
- Padovani, P., & Giommi, P. 1995, *MNRAS*, 277, 1477
- Padovani, P., & Giommi, P. 1996, *MNRAS*, 279, 526
- Padovani, P., Perlman, E. S., Landt, H., Giommi, P., & Perri, M. 2003, *ApJ*, 588, 128
- Sambruna, R. M., Maraschi, L., & Urry, C. M. 1996, *ApJ*, 463, 444
- Scarpa, R., & Falomo, R. 1997, *A&A*, 325, 109
- Schachter, J. F., Stocke, J. T., Perlman, E., et al. 1993, *ApJ*, 412, 541
- Stern, B. E., & Poutanen, J. 2008, *MNRAS*, 383, 1695
- Stocke, J. T., Liebert, J., Schmidt, G., et al. 1985, *ApJ*, 298, 619
- Stocke, J. T., Morris, S. L., Gioia, I. M., et al. 1991, *ApJS*, 76, 813
- Tavani, M., Barbiellini, G., Argan, A., et al. 2008, *Nuclear Instruments and Methods in Physics Research A*, 588, 52
- Thompson, D. J., Bertsch, D. L., Fichtel, C. E., et al. 1993, *ApJS*, 86, 629
- Urry, C. M., & Padovani, P. 1995, *PASP*, 107, 803
- Wang, J., Luo, Q., & Xie, G. 1996, *ApJ*, 457, L65
- Xie, G., Dai, B., Liang, E., Ma, L., & Jiang, Z. 2001a, *PASJ*, 53, 469
- Xie, G.-Z., Dai, B.-Z., Mei, D.-C., & Fan, J.-H. 2001b, *ChJAA (Chin. J. Astron. Astrophys.)*, 1, 213
- Xie, G. Z., Dai, H., Mao, L. S., et al. 2006, *AJ*, 131, 1210
- Xie, G. Z., Ding, S. X., Dai, H., Liang, E. W., & Liu, H. T. 2003, *International Journal of Modern Physics D*, 12, 781
- Xie, Z.-H., Dai, H., Hao, J.-M., Du, L.-M., & Zhang, X. 2007, *ChJAA (Chin. J. Astron. Astrophys.)*, 7, 209
- Xie, Z. H., Hao, J. M., Du, L. M., Zhang, X., & Jia, Z. L. 2008, *PASP*, 120, 477
- Xu, Y.-D., Cao, X., & Wu, Q. 2009, *ApJ*, 694, L107
- Zhang, J., Bai, J. M., Chen, L., & Liang, E. 2010, *ApJ*, 710, 1017
- Zheng, Y. G., Zhang, X., & Hu, S. M. 2007, *Ap&SS*, 310, 1